# A Comparison of NASA Scatterometer and ECMWF Winds and their Oceanic Response over the North Atlantic

Benny N. Cheng, Yi Chao, and W. Timothy Liu
Jet Propulsion Laboratory, California Institute of Technology

***Abstract***

Wind taken from the National Aeronautics and Space Administration (NASA) scatterometer (NSCAT) is compared with the operational analysis from European Center for Medium-Range Forecast (ECMWF) for the entire duration (about 9 months) of the NSCAT mission. Spectral analysis of the raw scatterometer data (along satellite swaths) shows a much higher energy content than that of the ECMWF analysis. To produce a gridded NSCAT wind suitable for driving ocean models, we adapt a Gaussian weighted window on the scatterometer wind and data gaps are filled in with the ECMWF wind. Spectral analysis of this blended product shows little energy difference from the ECMWF product in the range of 1000-500 km but a significantly higher energy content with spatial scale shorter than 500 km, and obeys the $k^{-2}$ power law well into the high wavenumber region. Both NSCAT and ECMWF winds are then used to drive an eddy-resolving North Atlantic Ocean model with a resolution of 1/6 degree and 37 vertical levels. Results show that in the Gulf Stream region both the NSCAT and ECMWF wind-driven model compare well with TOPEX data, while in the eastern subtropical region, the NSCAT wind-driven model simulates a more realistic synoptic variability of the sea surface height field.

## Introduction

Marine surface wind products distributed by numerical weather prediction (NWP) centers, such as the National Center for Environmental Prediction (NCEP) and ECMWF, are routinely used in the ocean modelling community for driving numerical models of the ocean (e.g. Barnier et al, 1991).

However, the wavenumber energy content of these analyzed winds follow the theoretical and measured $k^{-2}$ power law (Freilich and Chelton, 1986) only down to the spatial scale of 500 km. Due to the finite grid size of those NWP models and the approximation of subgrid-scale parametrization, it is found that the analyzed wind energy level below 500 km is much too weak compared to observations (Milliff et al, 1996). The satellite scatterometer wind measurements, on the other hand, have widely spaced and uneven spread of swath patterns, and therefore have to be interpolated between swaths before it can be used for driving ocean models. Simulations have shown that a better wind product should have a positive impact on the oceanic response in describing the general circulation and its variability (Milliff et al, 1996, Chin et al, 1997).

In this article, level 2.0 scatterometer wind data obtained from NSCAT (JPL, 1997) at 10-m height is first compared with ECMWF data (1° x 1° at 10-m level) and a Gaussian weighted gridding scheme is then applied to capture the high wavenumber wind energy that is previously missing from the operational winds (Milliff et al, 1996). The resulting wind field and the original ECMWF wind are then used to force an ocean general circulation model (OGCM) and the results are compared with TOPEX/POSEIDON observations to determine the impact of the NSCAT wind on simulating the North Atlantic ocean circulation and its variability.

## A Comparison Between NSCAT and ECMWF Winds

Our analysis of the NSCAT winds begins with a power wavenumber spectrum of the along-track wind data covering the entire period of the NSCAT mission from 9/15/96 to 6/30/97. We will be concerned only with the spectrum of zonal wind component, as our studies and others (e.g. Freilich and Chelton, 1986) have shown that the meridional component have similar properties. The region of interest concerns the Atlantic ocean starting from 100°W to 20°E and 35°S to 80°N. No distinction is made between the ascending and descending tracks in the calculation, as our analysis shows no sig-

nificant deviation from symmetry. Let $U_{NS}(x,t)$ denote a zonal NSCAT wind value at location $x$ and time $t$, where $t$ is assumed constant on a swath (recall that the satellite flies through the region very quickly on each cycle). A mean time-independent 1-d spatial autocovariance function $C(r)$ for this region is computed by taking all products of lag distance $r$ (spherical distance) along satellite tracks and then averaging over all time $t$, i.e.

$$C(r) = \mathbf{E}_t[(U_{NS}(x,t)-\mathbf{E}_x[U_{NS}(x,t)])(U_{NS}(y,t)-\mathbf{E}_y[U_{NS}(y,t)])], \ \text{dist}(x,y)= r. \qquad (1)$$

Here E denotes the averaging or expectation operator. A standard Hanning window is then applied to the covariance function before taking the fast Fourier transform (fft) to account for the finite size of the dataset. The resulting power spectrum and its corresponding chi-square 95% confidence interval is shown in Figure 1. The spectrum shape generally follows the well-known $k^{-2}$ slope for wind speed log power spectrum (Freilich and Chelton, 1986), up to about 500km. For wind scales less than 500 km, the slope becomes flat, and this increase in energy is consistent with the usual behavior expected from a noise-dominated spectral tail. We then compare this NSCAT spectrum with that obtained from ECMWF analysis in the same region and identical time period (see Figure 1). Since ECMWF wind are gridded, computation of the 1-d zonal wind spectrum are relatively easier and follows by taking the fft of the time-independent 1-d spatial autocovariance function along the zonal direction. The result clearly shows that raw NSCAT wind spectrum is more energetic, especially in the high wavenumber region having spatial scales of 500 km or less.

Judging from these observations, we are motivated to search for a gridded NSCAT wind product that would capture this extra energy seen in the scatterometer. A simple piece-wise (constant in time) interpolation scheme (Barnier et al, 1994) often retains clear swath patterns, while successive correction schemes that employ smoothing of the data (Tang and Liu, 1996; Liu et al, 1998) can weaken the high wavenumber energy content of the actual wind power if it is done too aggressively.

In this study, we experimented with grids having Gaussian weight with variable window size and scale. Let $X=(x,y,t)$ denote the space-time location of an NSCAT point, with wind speed $u(X)$. If $X_0=(x_0,y_0,t_0)$ denote a grid point, then

$$u(X_0) = \frac{\int_{X-W}^{X+W} u(X)\exp\left[-\ln(2)\left\|\frac{X-X_0}{S}\right\|^2\right]dX}{\int_{X-W}^{X+W} \exp\left[-\ln(2)\left\|\frac{X-X_0}{S}\right\|^2\right]dX} \qquad (2)$$

where $S=(sx,sy,st)$ is the scale factor and $W=(wx,wy,wt)$ is the window size. The scale parameter $S$ and the window size parameter $W$ are variables to be adjusted to produce as smooth as possible (eliminating satellite track patterns) a grid while not damping too much the energies in the high wavenumber region of the wind power spectrum. After some experimentations, we decided that the following values of $W=(1°,1°,2.day)$ and $S = (0.2°,0.2°,1.\ day)$ are appropriate for a resolution of 1° x 1° x 2 day. The remaining missing values (less than 10% of the points over water) were then substituted with ECMWF values to provide a uniform grid of wind values. As can be seen from a typical synoptic scale plot in Figure 2, the gridded NSCAT wind speed and direction can differ dramatically from ECMWF wind on a regional basis. We also compare their time-averaged spectrum over the entire region in Figure 1 and observed that the spectral properties of this blended dataset does exhibit the required energy boost in the high wavenumber that is expected of the scatterometer derived wind fields (Liu et al, 1998). Moreover, the blended wind spectra continues to have the expected $k^{-2}$ power law well into the high wavenumber regions.

## The Response of the North Atlantic Ocean Circulation to NSCAT and ECMWF winds

The impact of this blended NSCAT wind field on the ocean circulation and variability is in-

vestigated through an eddy-resolving OGCM based on the Parallel Ocean Program (POP) developed at Los Alamos National Laboratory (Dukowicz et al., 1993). This ocean model evolved from the Bryan-Cox 3-dimensional primitive equations ocean model (Bryan, 1969; Cox, 1984), developed at NOAA Geophysical Fluid Dynamics Laboratory (GFDL), and later known as the Semtner and Chervin (1992) model or the Modular Ocean Model (MOM; Pacanowski et al., 1991). In addition to the code structure which is ideal for the use on the massively parallel computer, the POP model differs from the original Bryan-Cox formulation in that it removes the rigid-lid approximation and treats the sea surface height as a prognostic variable (i.e., free-surface), therefore can be directly compared with satellite altimetry observations, from TOPEX/POSEIDON for example.

The model domain covers the Atlantic basin from 35°S to 80°N and from 100°W to 20°E and is formulated on a spherical grid with horizontal resolution of approximately 1/6° (0.1875° in longitude and 0.1843° in latitude), and 37 vertical levels and integrated for a total of thirty years forced with climatological seasonal air-sea fluxes (see Chao et al., 1996 for a detailed description). With the September conditions at the end of this 30-year spinup as the initial conditions, two 290-day integrations have been carried out corresponding to the period of the NSCAT mission. Model output in the form of the synoptic sea surface height field are saved at 3 day intervals, and only the last 4 months (120 days) of SSH fields are analyzed. We emphasized that the only difference between these two integrations is the wind forcing, one from the gridded NSCAT as described in the previous section and the other from ECMWF analysis.

To study the synoptic ocean response, particularly in the mesoscale, we concentrate on two regions in the North Atlantic, the Gulf Stream region (region I) with coordinates 50W-70W, 30N-40N and the eastern subtropical region (region II) with coordinates 20W-40W, 10N-20N. For each region, measurements of the sea level variability are done as follows. Let $H(x,y,t)$ denote the sea surface height (SSH) field obtained from the model in a particular patch, where $x$ denotes the longitude, $y$ the latitude,

and $t$ is the time. The 1-d spatial variance function as a function of time $V(t)$, is computed by first removing the meridional mean and taking all products in the meridional direction and then averaging over x, i.e.

$$V(t) = \mathbf{E}_{x,y}[H(x,y,t)-\mathbf{E}_y[H(x,y,t)]]^2 \quad (3)$$

Under the assumption of isotropy, this is equivalent to the 1-d along-track variance function of a satellite sampling path through the patch. The TOPEX SSH variability function on the other hand, is computed by taking all satellite tracks (spatial resolution of 6.2 km) lying within 2 days of a given day, and taking the average 1-d spatial variance over these tracks. This time binning of the TOPEX SSH variance is necessary because TOPEX tracks are too few and not long enough to cover a patch for any given day.

Figure 3a shows the variance plot as a time series for the patch near the subtropical region at 20W-40W, 10N-20N. Clearly, NSCAT SSH variability is significantly higher than the ECMWF SSH variability by about 50%, and closer to the much higher TOPEX SSH variability. On the other hand in Figure 3b, the NSCAT SSH variability fit to TOPEX variability is comparable to that of the ECMWF , indicating that the NSCAT model did just as well as the ECMWF model in the Gulf Stream region. The corresponding time-averaged wavenumber spectrum of for these two patches are shown in Figure 4. It is clear that in the West African region significant variability shows up across all wavenumbers, whereas in the Gulf Stream, both model spectra fit the TOPEX computed spectrum quite well. The above results mirror previous model simulations with synthetic scatterometer winds, which also detected a significant impact in the eastern basin of the North Atlantic (Milliff et al., 1996). As a possible explanation for the observed differences between the two regions, it could be that the tropical circulation is more responsive to the wind forcing, while in the middle and high latitudes, the internal variability and heat flux or even the fresh-water flux are equally important as the wind forcing in

driving the ocean circulation.

## Summary

A new gridded wind product is created that is a hybrid between the recently collected NSCAT scatterometer wind and ECMWF operational wind. This dataset is shown to have a high energy content in the high wavenumber that is consistent with that observed from along-track spectral analysis of the NSCAT wind data, hence more realistic when compared with the weak highwavenumber energy content that is present in the ECMWF winds alone. This NSCAT wind product is then tested on an eddy-resolving Atlantic model with 1/6° resolution and 37 vertical levels, and its sea level response in the North Atlantic is compared with those derived from the same model with ECMWF wind forcing and validated with TOPEX SSH observations. Within an integration time period of 290 days equal to the entire duration of the NSCAT mission, an observed change in the synoptic sea level variability of about 40-50% was detected in the eastern subtropical region, indicating that NSCAT winds does provide significant impact for some regions with this ocean model.

## Acknowledgments

This research was carried out at the Jet Propulsion Laboratory (JPL), California Institute of Technology, under contract with the National Aeronautics and Space Administration (NASA). Support from the NSCAT project and the High Performance Computing and Communication (HPCC) project are acknowledged. Computations were performed on the 256-processor Cray T3D through the JPL Supercomputing Project. We thank Ralph Milliff at NCAR, Scott Dunbar, Carol Hsu, and Wendy Tang at JPL for technical discussions during the course of this project, and Paulo Polito, Victor Zlotnicki, and two anonymous reviewers for their comments on the original manuscript.

## References


Barnier, B., M. Bonkthir, and J. Verron (1991). Use of Satellite Scatterometer Wind Data to Force a General Circulation Ocean Model. *J. Geophys. Res.* **96**, 22025-22042.

Bryan, K., (1969). A Numerical Method for the Study of the World Ocean Circulation, *J. Comput. Phys.*, **4**, 1687-1712.

Chin, T., R. Milliff, and W. Large (1997). Multiresolution Analysis of Scatterometer Winds and High-wavenumber Wind-driven Effects on Ocean Circulation. *J. of Atmos. and Oceanic Tech.* (submitted).

Chao, Y., A. Gangopadhyay, F. O. Bryan, and W. R. Holland (1996).Modeling the Gulf Stream System, How Far from Reality ?, *Geophys. Res. Lett.*, **23**, 3155-3158.

Cox, M. D., (1984). A Primitive Equation, 3-dimensional Model of the Ocean, Ocean Group Tech. Rep. 1, Geophysical Fluid Dynamics Laboratory, Princeton, NJ, 143pp.

Dukowicz, J. K., R. D. Smith, and R. C. Malone, (1993). A Reformulation and Implementation of the Bryan-Cox-Semtner Ocean Model on the Connection Machine, *J. Atmos. and Oceanic Tech.*, **10**, 195-208.

Freilich, M.H., and D.B. Chelton (1986). Wavenumber Spectra of Pacific Winds Measured by the SEASAT Scatterometer. *J. of Phys. Ocean.* **16**, 741-757.

JPL, (1997). NASA Scatterometer Science Data Product User's Manual, Version 1.1, April 1997. 68pp.

Large, W.G., W.R. Holland, and J.C. Evans (1991). Quasi-geostrophic Ocean Response to Real Wind Forcing: The Effects of Temporal Smoothing. *J. of Phys. Ocean.* **21**, 998-1017.

Liu, W. T., W. Tang, and P. Polito (1998). NASA Scatterometer provides Global Ocean-surface Wind fields with more Structures than Numerical Weather Prediction. *Geophys. Res. Lett.*, **25**, 761-764.

Milliff, R.F., W.G. Large, W.R. Holland, and J.C. McWilliams (1996). The General Circulation Responses of a High-resolution North Atlantic Ocean Model to Synthetic Scatterometer Winds. *J. of Phys. Ocean.* **26**, 1747-1768.

Pacanowski, R., K. Dixon, and A. Rosati, (1991). Modular Ocean Model Users Guide, Ocean Group Tech. Rep. 2, Geophysical Fluid Dynamics Laboratory, Princeton, NJ.

Semtner, A. J., and R. M. Chervin, (1992). Ocean General Circulation From a Global Eddy-resolving Model, *J. Geophys. Res.*, **97**, 5493-5550.

Tang, W., and W. T. Liu, (1996). Objective Interpolation of Scatterometer Winds, JPL Publ. 96-19, 16pp.

## Figure Captions

Figure 1. Power wavenumber spectra from NSCAT along-track zonal wind (red), ECMWF zonal wind (green), and gridded NSCAT blended with ECMWF wind (blue). The 95% confidence interval is computed from the original NSCAT along-track data.

Figure 2. (a) Gridded NSCAT winds and (b) ECMWF winds on January 15, 1997.

Figure 3.(a) Variance plot of the eastern subtropical region (20W-40W,10N-20N) as a function of time (b) Corresponding variance plot for the Gulf Stream region (50W-70W,30N-40N). Red color indicates the SSH variability of the NSCAT-driven model, green that of the ECMWF-driven model, and black represents the SSH variability computed from TOPEX/POSEIDON along-track data. 95% confidence envelope for the TOPEX SSH variability given as dotted lines.

Figure 4. (a) Wavenumber spectrum for the West Africa region averaged over the last 4 months of the integration time. (b) Corresponding wavenumber spectrum for the Gulf Stream region. Red color indicates the SSH spectrum of the NSCAT-driven model, green that of the ECMWF-driven model, and black represents the SSH spectrum computed from TOPEX/POSEIDON along-track data. 95% confidence interval is computed based on TOPEX SSH spectrum.

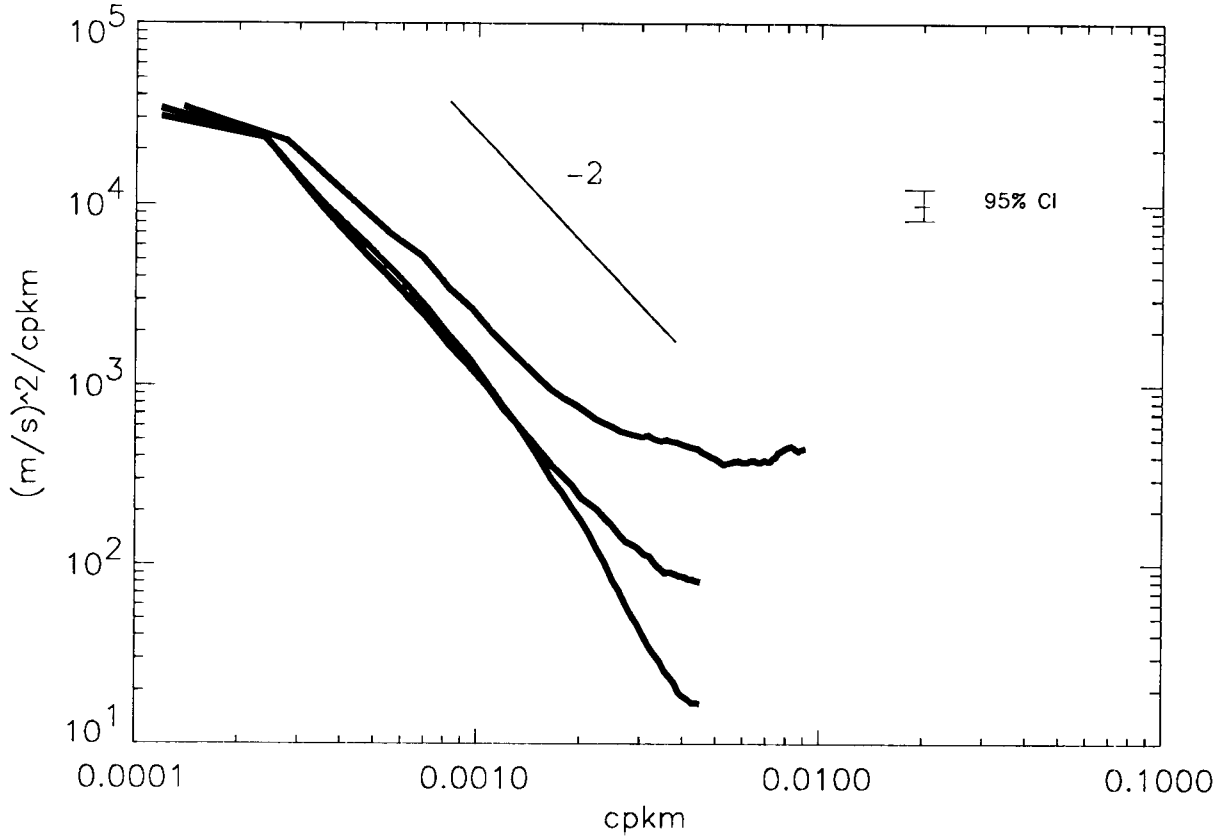
$10^5$
$10^4$
$10^3$
$10^2$
$10^1$
(m/s)^2/cpkm
-2
95% CI
0.0001
0.0010
0.0100
0.1000
cpkm

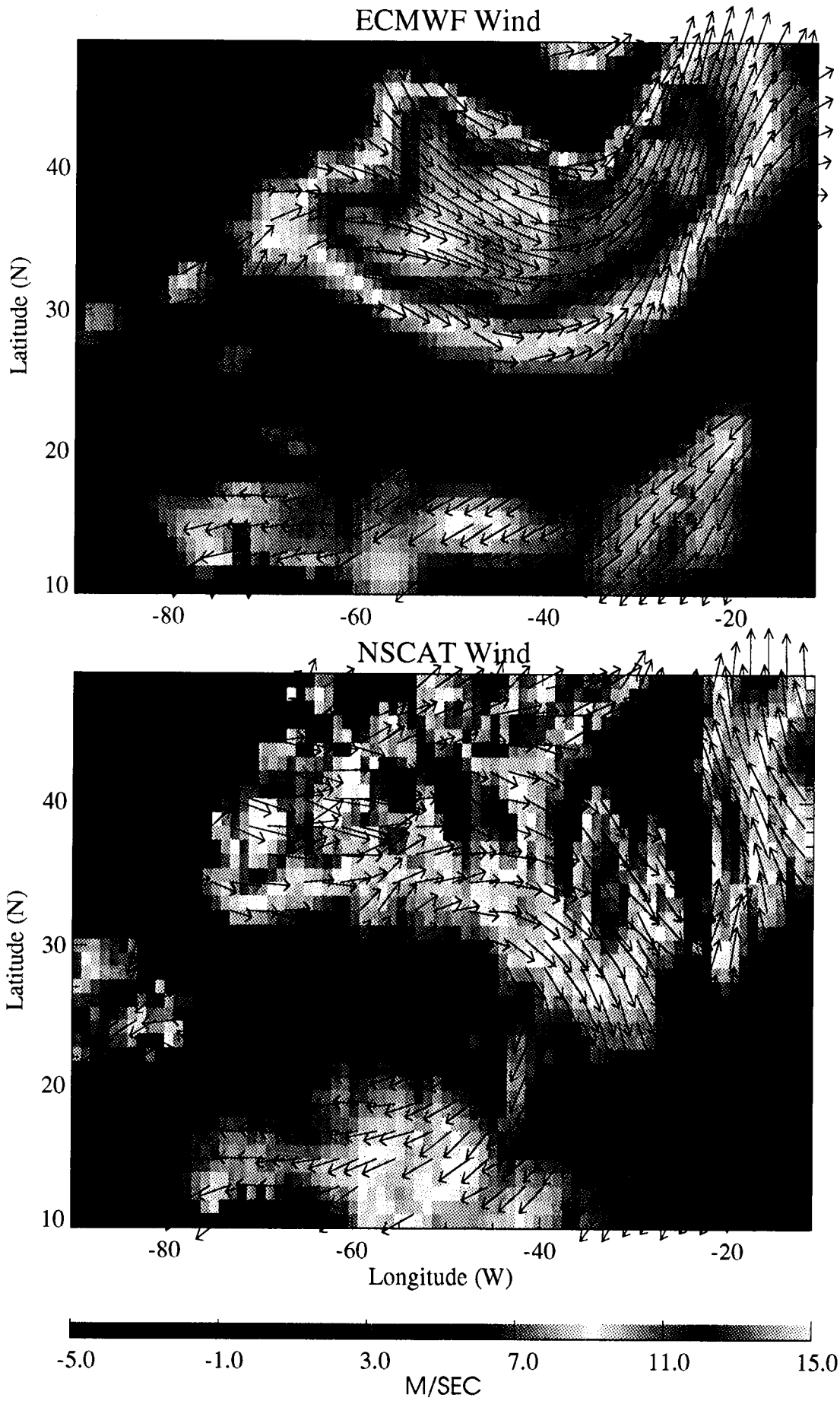
ECMWF Wind
40
30
20
10
Latitude (N)
-80
-60
-40
-20
NSCAT Wind
40
30
20
10
Latitude (N)
-80
-60
-40
-20
Longitude (W)
-5.0
-1.0
3.0
7.0
11.0
15.0
M/SEC

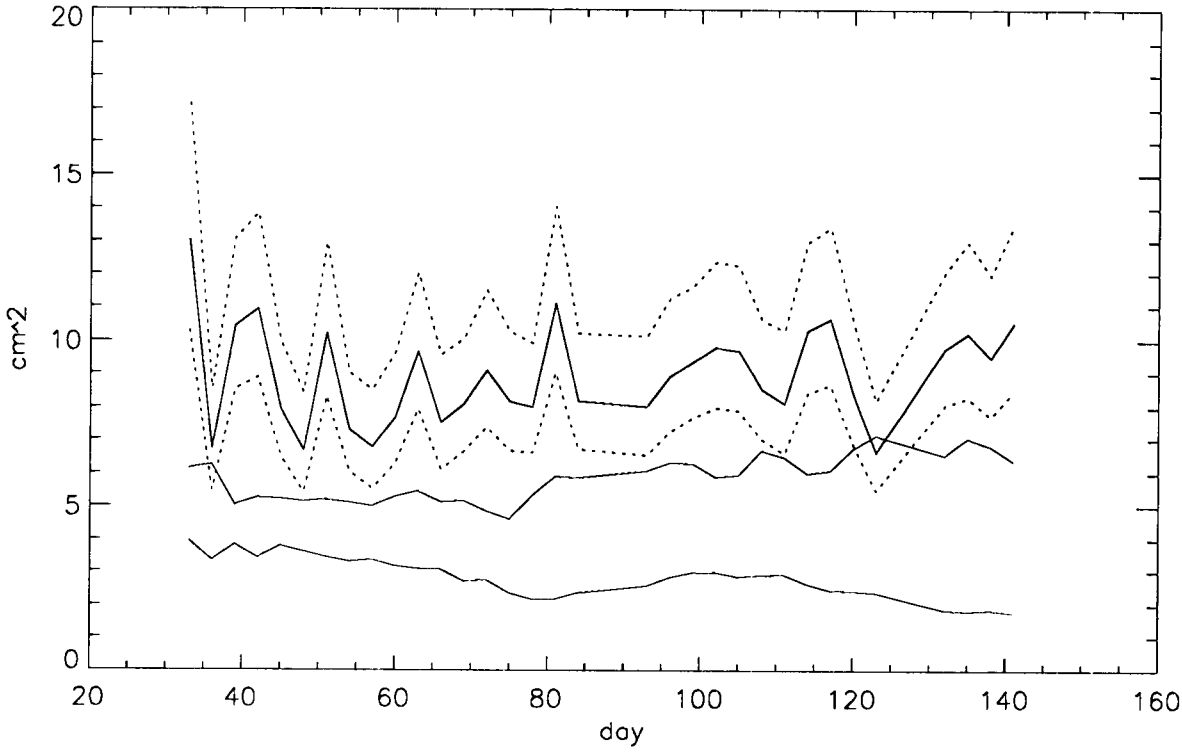


**Figure 3a.**

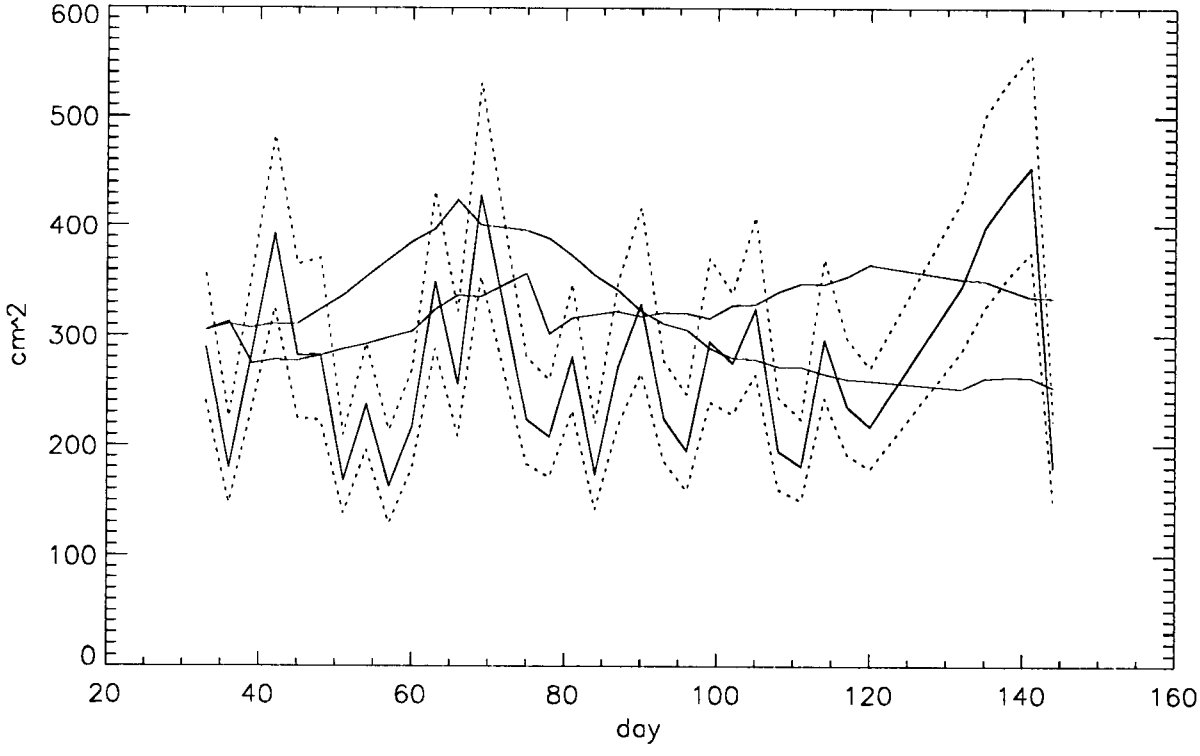


**Figure 3b.**

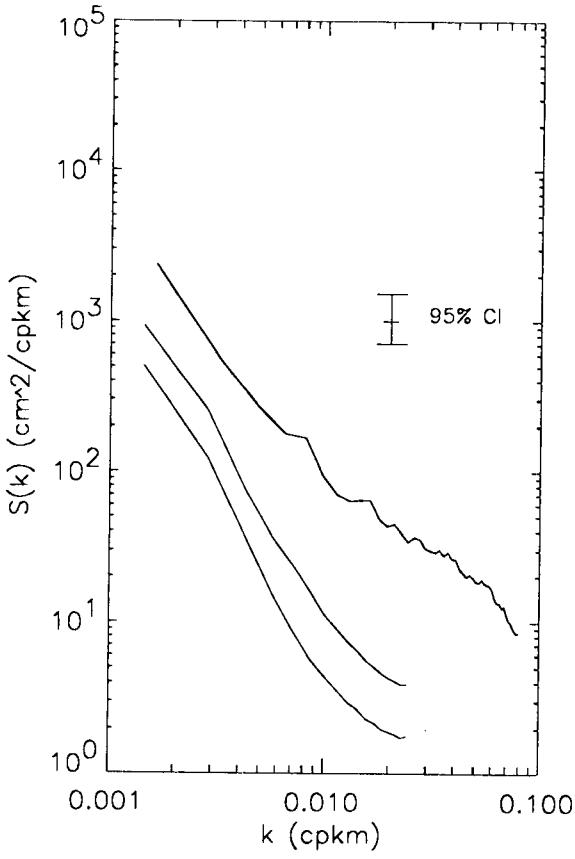


**Figure 4a.**

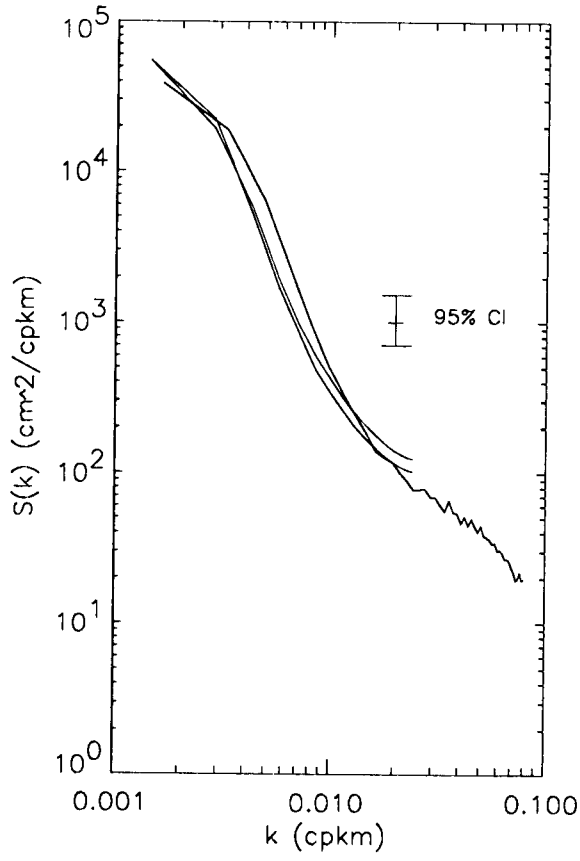


**Figure 4b.**